Proceedings of the SEM Annual Conference
June 1-4, 2009 Albuquerque New Mexico USA

Dynamic and Quasi-static Measurements of PBXN-5 and Comp-B Explosives

Geoffrey W. Brown[1,a], James A. Tencate[2], Racci DeLuca[1], Philip J. Rae[3], and Steven N. Todd[4]

[1]High Explosives Science & Technology (DE-1), [2]Earth & Environmental Sciences (EES-17), [3]Materials Science & Technology (MST-8), Los Alamos National Laboratory, Los Alamos, NM

[4]Energetic Systems Research (5916) and Systems Assessment and Research Center (5900), Sandia National Laboratories, Albuquerque, NM

[a]Corresponding author: MS C920, Los Alamos National Laboratory, Los Alamos, NM 87545.
email: geoffb@lanl.gov

ABSTRACT

We have measured dynamic and quasi-static mechanical properties of PBXN-5 and Comp-B explosive materials to provide input data for modeling efforts. Dynamic measurements included acoustic and split-Hopkinson pressure bar tests. Quasi-static testing was done in compression on a load frame. Split-Hopkinson and quasi-static tests were done at five temperatures from -50°C to 50°C. Our results were dominated by the low density of the samples. Acoustic velocities and strengths were low, as compared to other materials of the same or similar formulations. The data do provide useful input to materials models that include density as a parameter but suggest caution when using measurements of ideal materials to predict behavior of damaged materials.

INTRODUCTION

We have measured the strain-dependent mechanical properties of PBXN-5 and Comp-B explosive materials to provide input data for a Damage-Induced Reaction Model [1] (DMGIR) that has been used to predict non-shock-induced initiation. As in the development of other physics codes, the mechanical property data measured here contribute to constitutive relations that are used in equation-of-state models implemented in the code. PBXN-5 and Comp-B are relevant materials for DMGIR because they are present in a number of different types of munitions and because they can be considered representative “pressed” and “cast” explosive materials, respectively, to evaluate model capabilities.

EXPERIMENT

We measured dynamic and quasi-static mechanical properties of both materials. Dynamic measurements were made using split-Hopkinson pressure bar (SHPB) and acoustic testing. Quasi-static testing was done in compression. All stresses and strains are reported as true stresses and true strains in this work since, due to the small strains supported by these brittle materials, engineering and true strains are almost identical.

Split-Hopkinson pressure bar (SHPB) tests were carried out with a custom made instrument [2] at a strain rate of 3000 +/- 200 s^{-1}. The bar has an environmental chamber around the sample region that maintains the sample at various temperatures between -50°C and 50°C during measurements. Maraging steel bars were used in these experiments. Over the +/- 50°C temperature range used in these experiments, the impedance of the Maraging steel changes negligibly. Molybdenum grease was used to lubricate the sample ends. Samples were tested at

-50°C, -25°C, 0°C, 25°C, and 50°C. SHPB samples for both materials were 0.125 inch thick disks, 0.250 inches in diameter.

Quasi-static testing was carried out on a commercial load frame (MTS model 880). Specimens were compressed between polished tungsten carbide platens lubricated with molybdenum grease to reduce end face confinement. The platens were heated or cooled and surrounding insulation provided control of the sample temperature during testing. Samples were tested at -50°C, -25°C, 0°C, 25°C, and 50°C. Quasi-static samples for both materials were 0.250 inch thick cylinders, 0.250 inches in diameter.

Acoustic wave velocities were measured using a time-of-flight method illustrated schematically in Figure 1. For each sample, the transit times of the initial peaks in the longitudinal and shear wave signals were measured both with and without the explosive sample in the transducer-delay bar stack. Knowing the sample thickness, the difference in transit times with and without the sample present then gives the acoustic wave velocity. Both brass and aluminum delay bars were used for all samples and all testing was done at room temperature with commercial transducers having 1 MHz resonance frequencies. To couple the transducers to the samples, light machine oil was used for longitudinal wave measurements and thickened honey was used for shear wave measurements. Acoustic samples for all materials were 0.375 inch thick disks, 1 inch in diameter.

In addition to measured longitudinal (V_l) and shear wave (V_s) velocities, we also report the bulk sound velocity (V_B). This quantity is calculated using equation 1 and assumes that the material is linear, homogeneous, and isotropic.

$$V_B = \sqrt{V_l^2 - 4V_s^2/3} \tag{1}$$

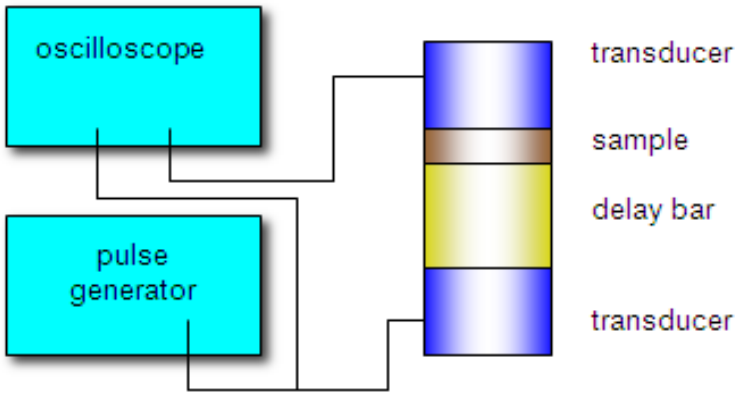

Figure 1. Schematic illustration of acoustic velocity measurement instrumentation.

SAMPLE MATERIALS

PBXN-5 is a plastic bonded explosive that is nominally 95% octahydrotetranitrotetrazine (HMX) by weight with 5% Viton-A binder. Viton-A is a commercial copolymer made of 60% vinylidine fluoride and 40% hexafluoropropylene. Typically, small prills of the PBXN-5 formulation are made in a slurry process and then the prill powder is pressed into billets that can be machined into desired shapes. The theoretical maximum density (TMD) of PBXN-5, based on the bulk density of its components, is 1.902 g/cc. Using immersion methods, we measured the density of the larger acoustic testing samples and found average densities of ~ 1.76 g/cc. We did not measure the densities of the individual samples for SHPB and quasi-static testing, but they were cut from the same pressed parts.

Comp-B is a melt-castable explosive nominally made up of 39.5% trinitrotoluene (TNT), 59.5% hexahydrotrinitrotriazine (RDX) and 1% wax, all by weight. The TMD of Comp-B is 1.737 g/cc. The samples used here were cut from larger parts cast in 2008. We measured the densities of the parts used for acoustic testing to be ~ 1.62 g/cc.

Finally, for acoustic testing only, we also measured samples of Comp-B that were cut from billets cast in 1960. The immersion densities for these older samples were ~1.72 g/cc.

RESULTS

PBXN-5 Results

The SHPB results for PBXN-5 at the temperature endpoints of +/- 50°C are shown in Figure 2. Each plot has traces from three different tests illustrating the sample-to-sample variability. Plots at -25°C, 0°C, and 25°C are not shown, but had very similar characteristics.

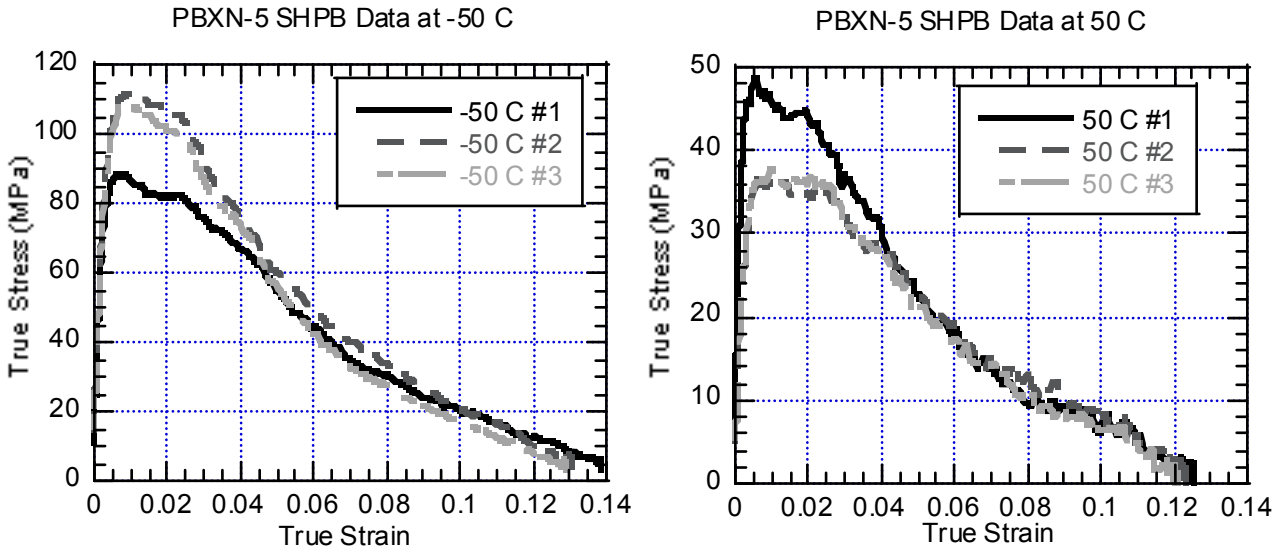

Figure 2. SHPB data from PBXN-5 at -50°C and 50°C.

An example of the equilibrium region of the PBXN-5 SHPB data can be seen from the "1-wave","2-wave" plots shown in Figure 3. "1-wave" traces are the transmitted bar signals while "2-wave" traces are the sums of synchronized incident and reflected bar signals [3]. Typically, SHPB data is a valid measurement of the sample properties in regions where the 2-wave signal oscillates around the 1-wave signal and where the strain rate is roughly constant. For the PBXN-5 data sets here, this region is roughly between 1.5% and 3.5% strain. Before 1.5% strain, the system has not reached equilibrium and after 3.5% strain, the signals are primarily related to damage accumulation in the sample. Example PBXN-5 SHPB data for all temperatures is also in Figure 3.

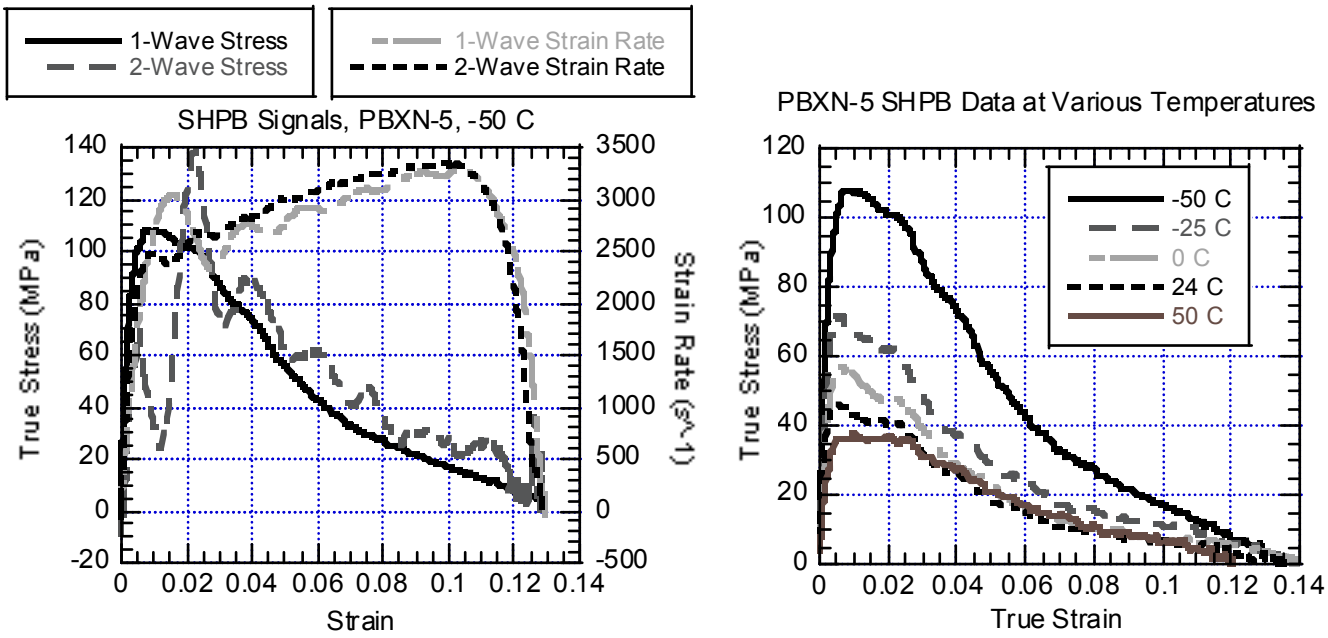

Figure 3. (left) SHPB stress and strains for one test on PBXN-5 at -50°C. (right) Compilation of representative SHPB data for PBXN-5 at all temperatures tested.

Quasi-static testing results for PBXN-5 at the temperature endpoints of +/- 50°C and at two different strain rates are shown in Figure 4. Each plot has traces from two different tests at each strain rate, illustrating the sample-to-sample variability. Plots at -25°C, 0°C, and 25°C are not shown, but had similar characteristics.

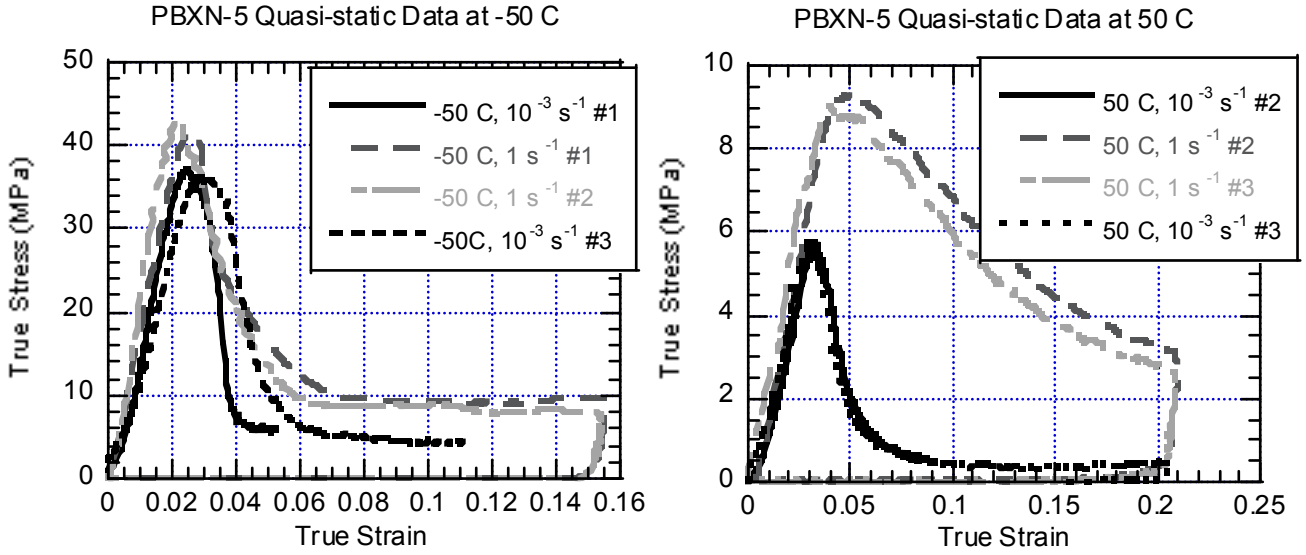

Figure 4. Quasi-static compression data for PBXN-5 at -50°C and 50°C.

Comp-B Results

The SHPB results for Comp-B at the temperature endpoints of +/- 50°C are shown in Figure 5. Each plot has traces from three different tests illustrating the sample-to-sample variability. Plots at -25°C, 0°C, and 25°C are not shown, but had similar characteristics.

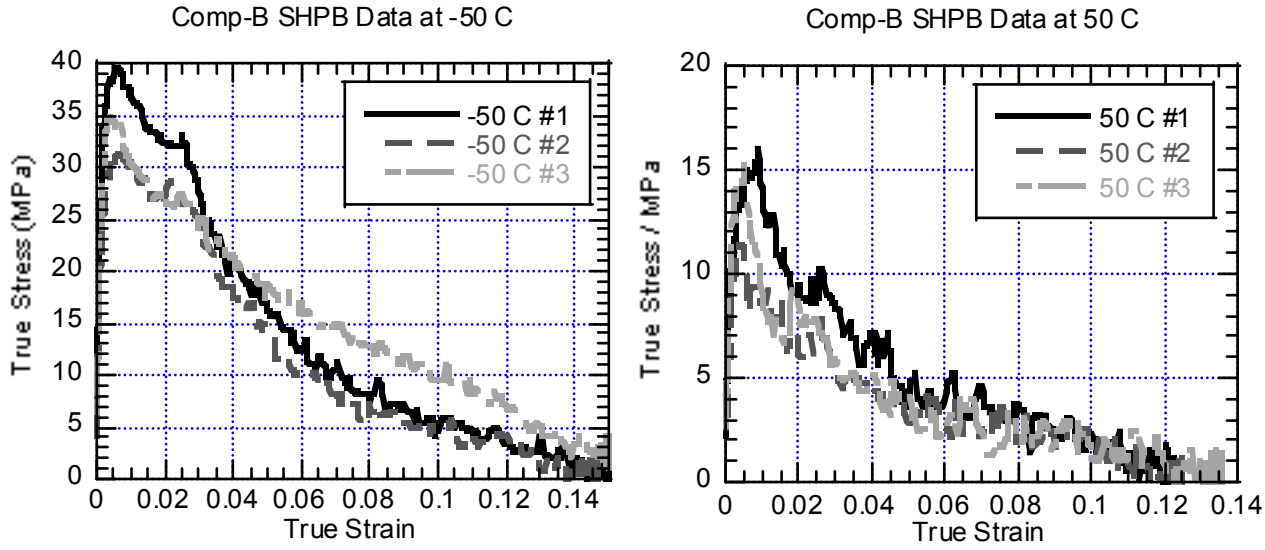

Figure 5. SHPB data from Comp-B at -50°C and 50°C.

The equilibrium region of the Comp-B SHPB data can be seen from “1-wave”-“2-wave” plots shown in the left panel of Figure 6 for the -50°C data set. For Comp-B, the equilibrium region is between 2.5% and 4% strain. Example Comp-B SHPB data for all temperatures is compiled in the right panel of Figure 6.

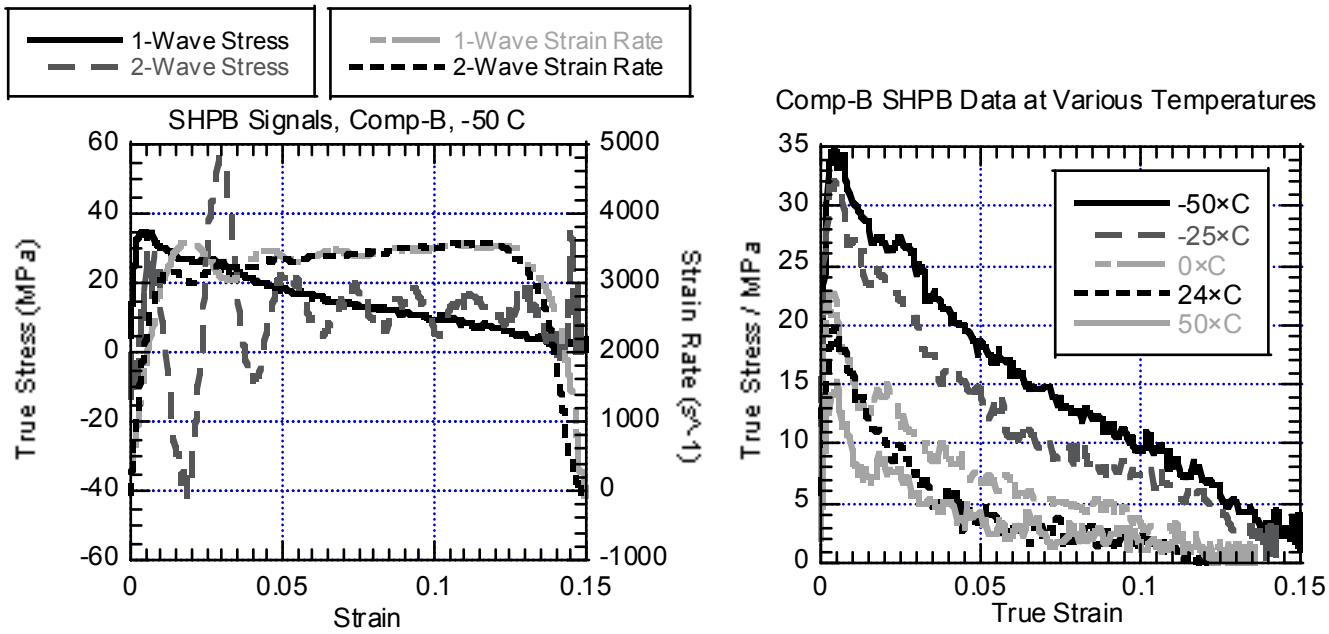

Figure 6. (left) SHPB stress and strains for one test on Comp-B at -50°C. (right) Compilation of representative SHPB data for Comp-B at all temperatures tested.

Quasi-static testing results for Comp-B at the temperature endpoints of +/- 50°C and at two different strain rates are shown in Figure 7. Each plot has traces from different tests illustrating the sample-to-sample variability. Plots at -25°C, 0°C, and 25°C are not shown, but had similar characteristics.

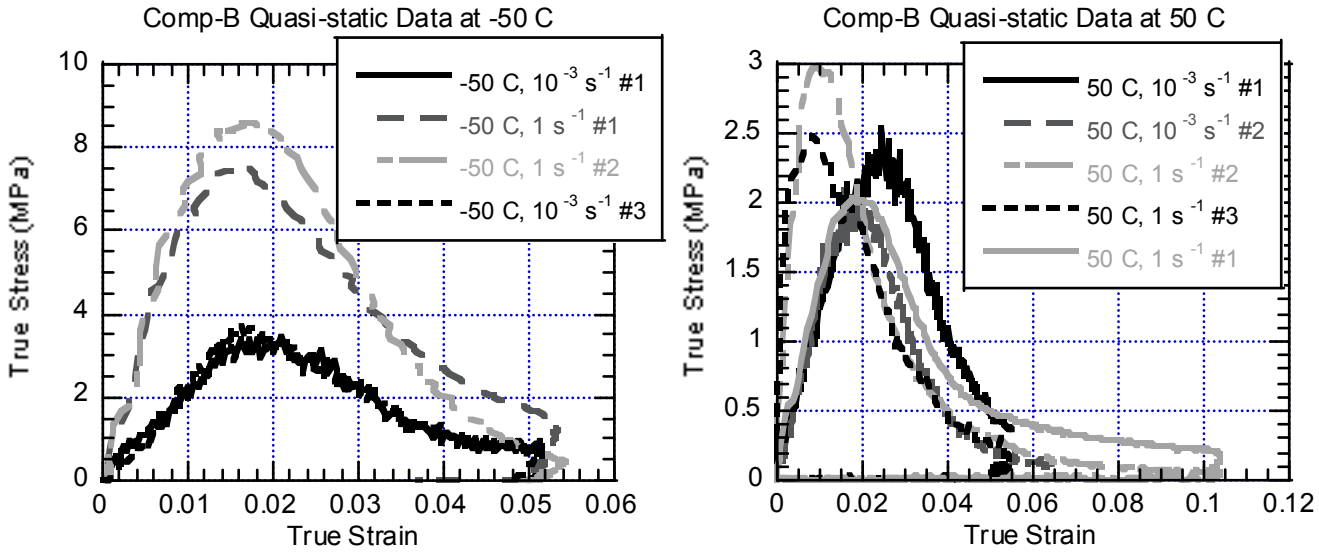

Figure 7. Quasi-static compression data for Comp-B at -50°C and 50°C.

Maximum stress data for both PBXN-5 and Comp-B at all temperatures and strain rates are compiled in Figure 8 as a function of temperature. For the SHPB data, PBXN-5 stress at 1.5% strain and Comp-B stress at 2.5% strain are plotted. At those strains, the 1-wave and 2-wave signals begin to coincide.

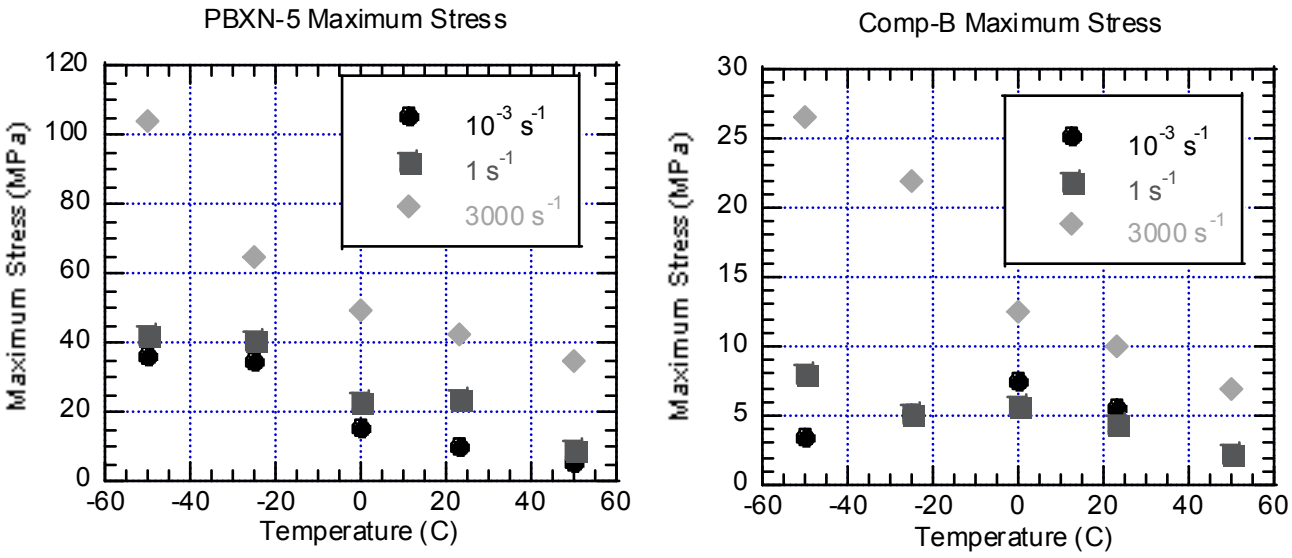

Figure 8. Maxmimum material stress for PBNX-5 (left) and Comp-B (right) as a function of temperature and strain rate.

Failure structures

PBXN-5 failed in a granular fashion in Hopkinson bar testing, leaving many small particles. Under lower strain rates in quasi-static testing, the PBXN-5 underwent cup and cone failures at each end. The diameter of the cones corresponded to the outside diameter of the samples. This indicates that the mode of failure is preferential cracking along regions of maximum shear.

Comp-B samples failed in a granular fashion in both testing modes.

Acoustic Results

Table 1 shows the acoustic velocities measured and calculated in this work and values quoted in other published studies for similar materials.

Table 1. Comparison of average densities and acoustic velocities measured here with published values for similar materials. Values from this work are in bold. Uncertainties on values measured in this work, estimated from variability in repeated measurements, are +/- 0.001 g/cc and +/- 0.04 km/s.

Material	Density (g/cm^3)	V_l (km/sec)	V_S (km/sec)	V_B (km/sec)	Reference
PBXN-5	**1.762**	**1.85**	**1.10**	**1.35**	**This Work**
PBXN-5	1.85			2.1	4
PBX 9501 [a]	1.82	2.97	1.39	2.50	5
New Comp B	**1.617**	**1.98**	**1.16**	**1.46**	**This Work**
Old Comp B	**1.721**	**3.08**	**1.60**	**2.46**	**This Work**
Comp-B3 [b]	1.70	3.00	1.62	2.35	5
Comp-B	1.715	3.12	1.71	2.42	6

[a] PBX 9501 is 95% HMX by weight with 5% estane + nitroplasticizer as a binder.
[b] Comp-B3 is the same formulation as Comp-B but does not include wax.

DISCUSSION

PBXN-5

All strain rates for PBXN-5 SHPB and quasi-static tests show an initial linear loading segment, little ductility, and rapid damage accumulation. At higher strain rates, the SHPB data shows a small amount of approximately constant flow stress before damage begins to accumulate. The glass transition temperature of the binder, in the vicinity of -20°C, obviously affects the strength of the material in quasi-static testing. There is only a weak glass transition effect on the SHPB data and the strengths measured at all strain rates tend to converge at higher temperatures as the binder softens.

The low strength of this material, relative to similar energetic composites such as PBX 9501, is likely due to the low density of the parts that were tested. As the porosity increases, the amount of solid material in the cross sectional area decreases and the material appears weaker. The high porosity may also account for the constant flow stress region observed in the SHPB data. Similar effects have been observed in porous metals [7,8] and packed explosive powders [9]. Qualitatively for our data, pore collapse could accommodate some amount of strain in the material before typical damage features appear and macroscopic stress-relieving cracks grow across the sample. It is also possible that the pore collapse regions themselves could coalesce into the stress relieving features. Their nucleation and growth would be inhibited by the presence of the HMX crystals, allowing a more pervasive and uniform damage field to build up inside the material to form macroscopic features. This could account for the granular failure of PBXN-5 in the SHPB measurements.

Comp-B

Interpretation of the Comp-B results is qualitatively similar to that for PBXN-5, except for the lack of a constant flow stress region in the SHPB data and the lack of glass transition effects since Comp-B has no binder. The strengths at all strain rates do tend to converge at higher temperatures, likely because the melting point of Comp-B is near 85°C. In keeping with the qualitative arguments presented above, the lack of constant flow stress in Comp-B could be due to the homogeneous nature of this melt-cast material. For example, since there is no binder/crystal structure to interfere with nucleation and growth of pore-collapse damage regions, the regions can readily interact and form macroscopic structures that relieve stress.

A common feature of the data from both materials is lower than expected strain-rate dependence of the maximum mechanical strength during quasi-static testing. This may also be explained by the porosity of the samples if stress concentration in the pores and damage due to pore collapse dominate the low strain rate damage accumulation and thereby largely determine the mechanical strength of the material.

Acoustic Results

The acoustic velocities measured here for PBXN-5 and the new Comp-B samples are low, but not unexpected, again given the low density of this material. As seen in Table 1, old Comp-B samples near TMD show high acoustic velocities, as do Comp-B3 samples. In acoustic testing, porosity leads to lower wave velocity since the speed of sound in air is slower than that in the solid material.

SUMMARY

We have measured the dynamic and quasi-static mechanical properties of PBXN-5 and Comp-B explosive materials. The properties reflect the low density of the samples and are qualitatively consistent with the presence of pores and effects due to pore collapse. The data reported here will be useful as input to the DMGIR model or other codes that employ constitutive relations. It should be noted, however, that our measurements are only valid for the low density materials that we tested. As a result, application of these results to predict behavior of nominal density materials will not be a straightforward process.

REFERENCES

[1] Todd, S.N., Vogler, T.J., Caipen, T.L., and Grady, D.E., "Non-shock initiation model for plastic bonded explosive PBXN-5: Theoretical Results", *Shock Compression of Condensed Matter – 2007*, CP955, pp. 1006 – 1009, 2007.

[2] Gray III, G.T., and Blumenthal, W.R. "Split-Hopkinson pressure bar testing of soft materials", ASM Handbook, *Volume 8 – Mechanical Testing and Evaluation*, ASM International, pp. 488 – 496, 2000.

[3] Gray III, G.T., Idar, D.J., Blumenthal, W.R., Cady, C.M., and Peterson, P.D., "High-and-low strain rate compression of several energetic material composites as a function of strain rate and temperature", *11th International Detonation Symposium*, 1998.

[4] Chen, P., Huang, F., Dai, K., and Ding, Y., "Detection and characterization of long-pulse low velocity impact damage in plastic bonded explosives", *Int. J. Impact Eng.* Volume 31, pp. 497, 2005.

[5] Olinger, B., and Hopson, J.W., "Dynamic properties of some explosives and explosive simulants", *Proceedings of the Symposium on High Dynamic Pressures*, Paris, pp. 9-19, 1978.

[6] Marsh, S., LASL Shock Hugoniot Data, Univ. Calif. Press, Berkeley, CA, 1980.

[7] Hakamada, M., Yamada, Y., Nomura, T., Kusuda, H., Chen, Y., and Mabuchi, M., "Effect of sintering temperature on compressive properties of porous aluminum produced by spark plasma sintering", *Materials Transactions*, volume 46, pp. 186 – 188, 2005.

[8] Hasegawa, T., and Yakou, T., "'Region of constant flow stress' during compression of aluminum polycrystals prestrained by tension", *Scripta Metallurgica*, volume 8, pp. 951 – 954, 1974.

[9] Lowe, C.A., and Longbottom, A.W., "Effect of particle distribution on the compaction behavior of granular beds", Physics of Fluids, volume 18, pp 066101 - 066116, 2006.